



Proceedings of the Seventeenth International Conference on
Civil, Structural and Environmental Engineering Computing
Edited by: P. Iványi, J. Kruis and B.H.V. Topping
Civil-Comp Conferences, Volume 6, Paper 11.10
Civil-Comp Press, Edinburgh, United Kingdom, 2023
doi: 10.4203/ccc.6.11.10
©Civil-Comp Ltd, Edinburgh, UK, 2023

Seismic Energy Dissipation Analysis of a Low-Rise Steel Structure with Buckling Restrained Braces

H. Yang^{1,2} and B. Jeremić^{3,4}

¹School of Civil Engineering, Tianjin University, China

²National Facility for Earthquake Engineering Simulation,
Tianjin University, China

³Department of Civil and Environmental Engineering,
University of California, Davis, USA

⁴Earth and Environmental Sciences Area,
Lawrence Berkeley National Laboratory, USA

Abstract

This paper presents a numerical study on seismic energy dissipation in a steel frame structure featuring buckling restrained braces (BRBs) for seismic protection. The Real-ESSI Simulator is used to construct a nonlinear finite element model of a two-story building that was designed by following ASCE-7 guidelines. The numerical model also features a spread foundation, underlying soil layers, and the soil-foundation interface. The model is excited by seismic motion that has two orthogonal components in the horizontal plane. Eigen analysis and dynamic time domain analysis are performed and discussed. The distribution and evolution of energy dissipation within the system is analysed. Of particular interest is the performance of the BRBs during a seismic event, in terms of their ability to dissipate seismic energy.

Keywords: seismic energy dissipation, finite element method, buckling restrained braces, soil structure interaction, nonlinear analysis, low-rise steel structure

1 Introduction

Seismic events pose a significant threat to the safety and stability of structures, necessitating the development of effective seismic protection strategies. One approach to enhancing the seismic performance of buildings is through the use of buckling

restrained braces (BRBs), which are capable of dissipating seismic energy and reducing the forces transmitted to the structure [1,2]. This paper presents a comprehensive numerical study on the seismic energy dissipation analysis of a low-rise steel structure reinforced with buckling restrained braces.

Energy dissipation has been proven to be an effective parameter in evaluating material damage and seismic performance of structures and soil structure interaction (SSI) systems. One advantage of energy dissipation over traditional design parameters is that energy dissipation continuously accumulates as material is being damaged during a seismic event [3]. As pointed out by Yang et al. [4], in an SSI system under seismic loading, the two physical energy dissipation mechanisms are material inelasticity and viscous coupling. Note that the energy dissipation caused by material inelasticity, or plastic energy dissipation, is the term that indicates damage if it is observed in structural members, and energy dissipation in soil domain and foundation-soil interfaces. It should also be pointed out that algorithmic damping, which is used to achieve stable simulation result, should be applied with care as it could overshadow the physical energy dissipation mechanisms [5,6].

The objective of this study is to analyse the seismic energy dissipation within a low-rise steel structure equipped with buckling restrained braces. To achieve this, a numerical model is developed using the Real-ESSI Simulator, a software, hardware, and documentation system for high performance nonlinear finite element modelling and simulation of earthquake, soil, structure, and their interaction [7]. The structural model represents a two-story steel building designed in accordance with the guidelines outlined in ASCE 7 standards. In addition to the building structure, the numerical model incorporates essential components such as spread foundations, underlying soil layers, and the soil-foundation interface.

In the following sections, the formulations for energy dissipation due to material inelasticity and viscous damping are summarized. Next, the modelling techniques and details used in this paper are introduced. The dynamic response of the SSI system is presented. The energy dissipation results of the model, particularly that in the BRBs, are presented and discussed.

2 Theory and Formulation

The energy computation approach used in this paper is developed based on principles of thermodynamics and classic elastoplasticity theory. Detailed derivation and explanation of the theoretical framework can be found in a previous publication [4]. Here, only equations relevant to this work are presented.

2.1 Plastic Energy Dissipation

Based on the first and second laws of thermodynamics, the local form of plastic energy dissipation density was given by Yang et al. [4] as

$$\Phi = \sigma_{ij} \Delta \epsilon_{ij}^{pl} - \Delta \Psi^{pl} \quad (1)$$

where Φ is the incremental plastic energy dissipation density, σ_{ij} is the stress tensor, ϵ_{ij}^{pl} is the incremental plastic strain tensor, and Ψ^{pl} is the incremental plastic free

energy density. Note that, according to the second law of the thermodynamics, the incremental plastic energy dissipation should always be nonnegative.

According to Equation (1), plastic free energy needs to be defined so that plastic dissipation can be calculated. Yang et al. [8] pointed out that plastic free energy is associated with material microstructure or fabric, thus should be calculated using the internal variables, or state variables, of the corresponding constitutive model.

In this work, the soil material is modelled using a non-associated hyperbolic Drucker-Prager plasticity model, for which the incremental plastic free energy density was derived by Yang et al. [9] as

$$\Delta\Psi^{pl} = \left(\frac{3}{2h_a} \alpha_{ij} \Delta\alpha_{ij} - m_{ii}^{vol} \Delta\lambda \right) p \quad (2)$$

where h_a is a hardening constant, α_{ij} is an internal variable usually referred to as the back stress, m_{ii}^{vol} is the volumetric part of the normalized plastic flow direction tensor, $\Delta\lambda$ is the scalar loading index, and p is the mean stress or hydrostatic pressure.

The nonlinear component of the BRBs is modelled using a uniaxial steel fibre material model [11,12], for which the incremental plastic free energy density was derived by Yang et al. [10] as

$$\Delta\Psi^{pl} = \frac{1}{2} [(\sigma + \sigma_r) \Delta\epsilon + (\epsilon_{pl} - \epsilon_r) \Delta\sigma] \quad (3)$$

where σ and ϵ are the current stress and strain, σ_r and ϵ_r are the stress and strain at the point of strain reversal, and ϵ_{pl} is the plastic strain.

2.2 Viscous Damping

In this work, the viscous coupling between solids and fluids is captured using Rayleigh damping. The incremental energy dissipation caused by viscous damping ΔD_v , was given by Yang et al. [5] as

$$\Delta D_v = (a_M M_{ij} + a_K K_{ij}) \dot{u}_i \Delta u_i \quad (4)$$

where a_M and a_K are the damping coefficients, M_{ij} is the mass matrix, K_{ij} is the stiffness matrix, and u_i is the generalized displacement vector.

3 Modelling Procedure

The numerical model of the SSI system studied in this paper is shown in Figure 1. The model consists of a two-story steel structure with BRBs, spread foundation, underlying soil layers, soil-foundation interface, and surrounding layers for applying seismic motion.

3.1 Modelling of BRBs

The BRBs are modelled using a combination of linear elastic and nonlinear inelastic beam elements, which are readily available in the Real-ESSI Simulator. Laboratory experiments were conducted to determine the dynamic response of each BRB when a

cyclic normal load is applied. These test data is used to calibrate the numerical model of the BRBs used in this work. Figure 2 shows the comparison between test data and calibrated numerical response.

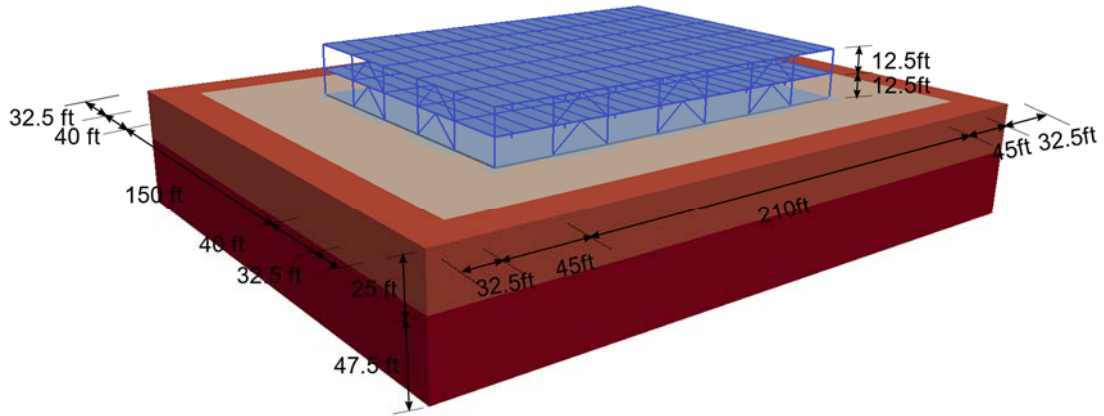


Figure 1: Numerical model of the SSI system (1 ft = 0.305 m).

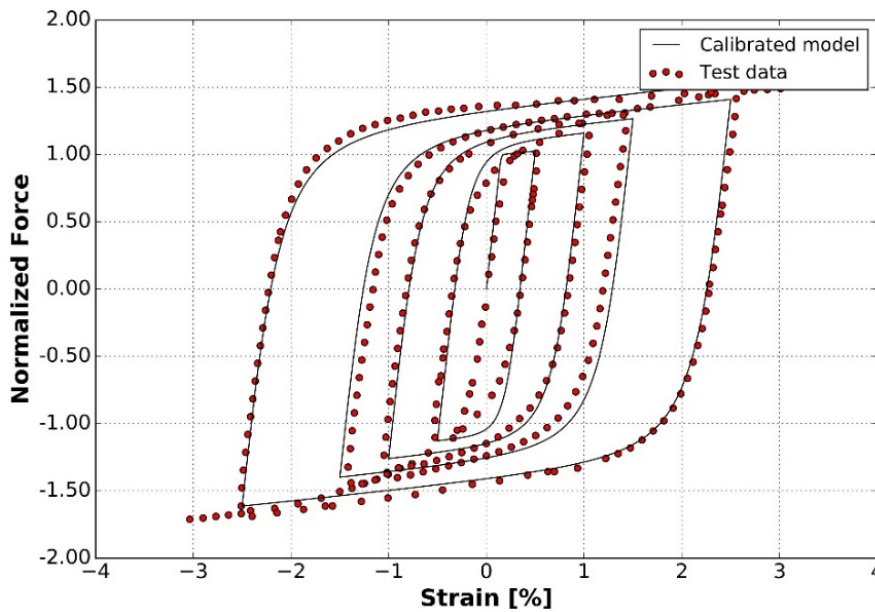


Figure 2: Calibration of the inelastic behaviour of the buckling restrained braces.

3.2 Modelling of Soil Layers

A realistic soil profile is chosen for this study. Based on the site investigation results shown in Figure 3, the underlying soil is divided into two layers.

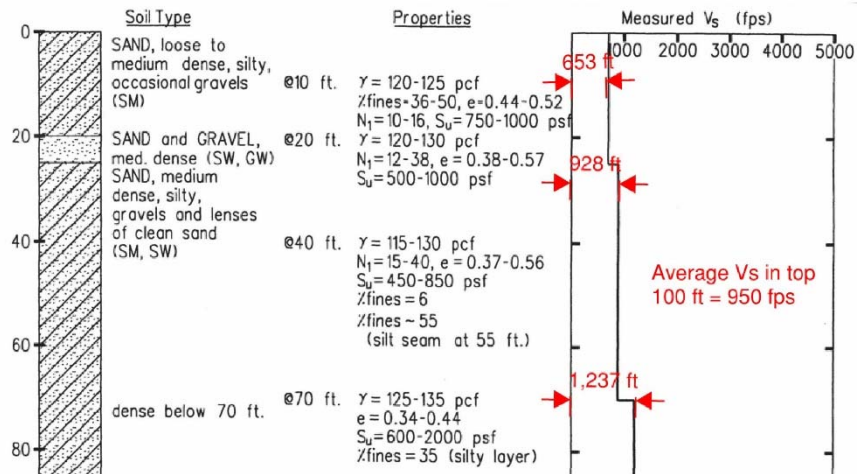
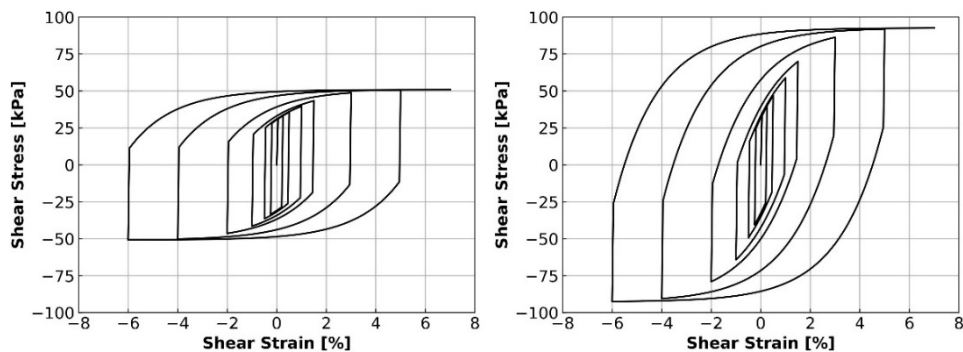


Figure 3: Site condition and material properties of the underlying soil layers (1 ft = 0.305 m, 1 pcf = 16.02 kg/m³, 1 psf = 47.88 N/m², 1 fps = 0.305 m/s).

Solid 8-node-brick elements and non-associated hyperbolic Drucker-Prager plasticity model are used to model the soil layers. The material model parameters are calibrated to match the shear strength data shown in Figure 3. The cyclic responses of the top and bottom soil layers are shown in Figure 4.



(a) Top Layer (Depth = 10 ft) (b) Bottom Layer (Depth = 50 ft)

Figure 4: Cyclic responses of the material model used for the soil layers.

3.3 Seismic Motion

Two horizontal components (2C) of earthquake records 120711 and 120712 are shown in Figure 5. The motions are scaled by a factor of 1.82 to match the design spectrum specified in ASCE 7 standards.

For seismic motion application, the domain reduction method (DRM) proposed by Bielak et al. [13] is used in this study. The acceleration and displacement time histories are used to construct a 3D wave field using the wave potential formulation approach developed by Wang et al. [14] that is available in Real-ESSI.

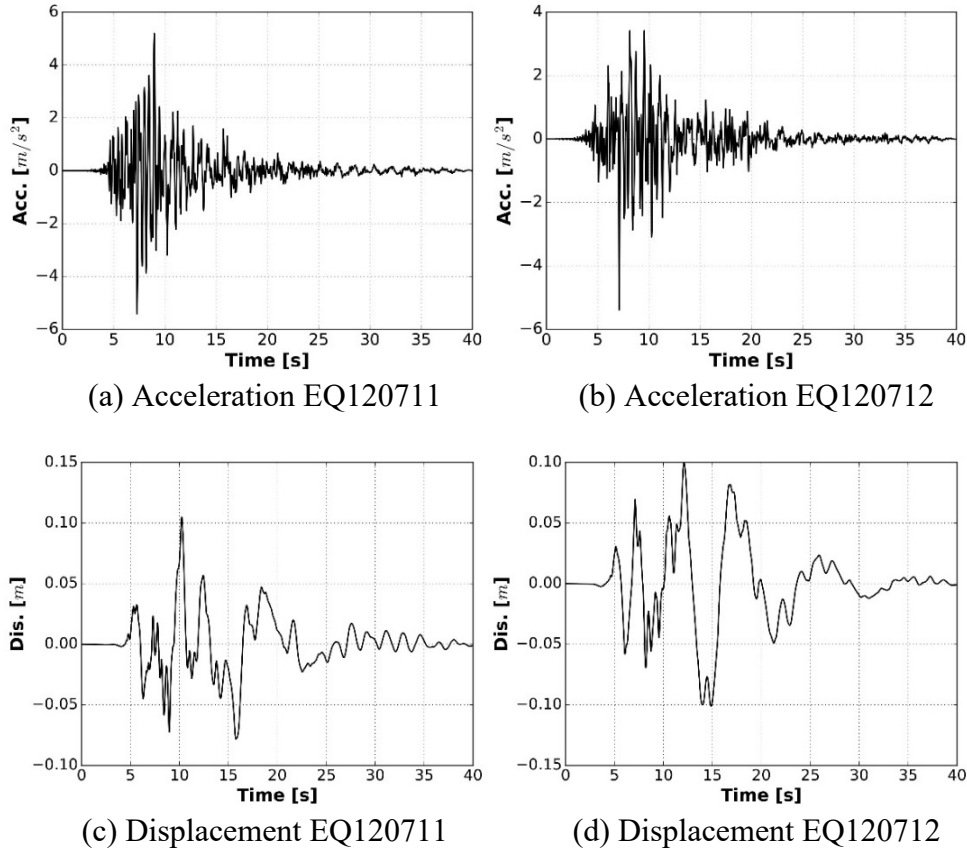


Figure 5: Earthquake motion records used in this study.

4 Numerical Results

4.1 Eigen Analysis

Eigen analysis was performed to check the model and to investigate the dynamic characteristics of the two-story steel building equipped with BRBs. The first 4 eigen modes of the model are presented in Figure 6. The first eigen mode shows a horizontal shear deformation along the direction of the short edge. Similarly, the second eigen mode shows the same type of deformation along the direction of the long edge. The third eigen mode is a twisting mode. The fourth eigen mode shows localized deformation on the top floor. Note that significant deformations are observed in the BRB elements for the first three eigen modes.

The first 7 eigen periods and frequencies of the building model are summarized in Table 1. The first three eigen frequencies fall in the range of the dominant frequency of the seismic motion used in this study. This means that the first three eigen modes are likely to be excited when the seismic motion is applied.

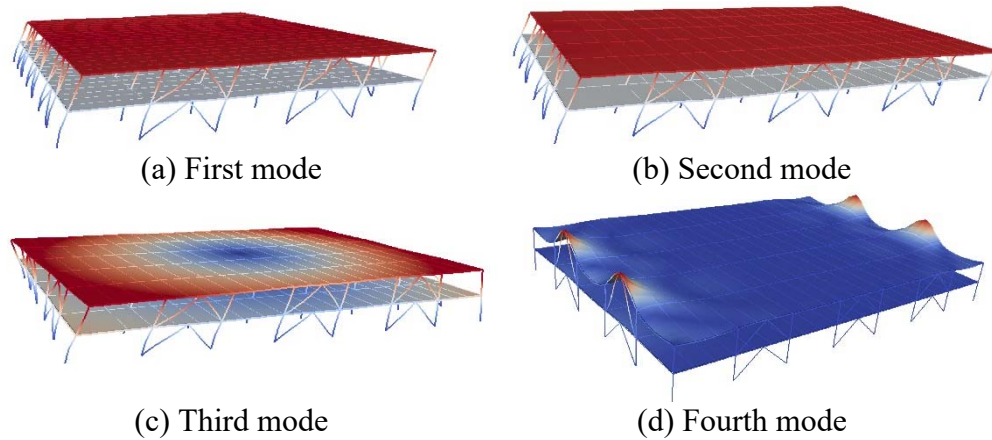


Figure 6: First 4 eigen modes of the steel building model.

Eigen Mode #	Eigen Period [s]	Eigen Frequency [Hz]
1	0.692	1.446
2	0.575	1.739
3	0.508	1.970
4,5	0.325	3.076
6,7	0.324	3.084

Table 1: First 7 eigen periods and frequencies of the steel building model.

4.2 Dynamic Response

The seismic motion shown in Figure 5 is applied to the SSI system model shown in Figure 1. To investigate the effect of plastic energy dissipation caused by inelastic materials in the SSI system, a model with linear elastic materials for all components is constructed and analysed. The dynamic responses at various locations of the structure are recorded and plotted in Figure 7. At the foundation level, the inelastic case shows significantly smaller accelerations than those seen in the elastic case. At the top floor, there is clear permanent deformation observed in the inelastic case.

According to Figure 7(c) and 7(d), the inelastic case, which includes the energy dissipating BRBs, shows slightly smaller accelerations but higher displacements than those from the elastic case. Based on the acceleration and displacement responses alone, it is not clear how effective the BRBs are in protecting the structure during an earthquake. In the next section, the plastic energy dissipation in the SSI model is analysed to provide more insight into the seismic performance of the BRBs.

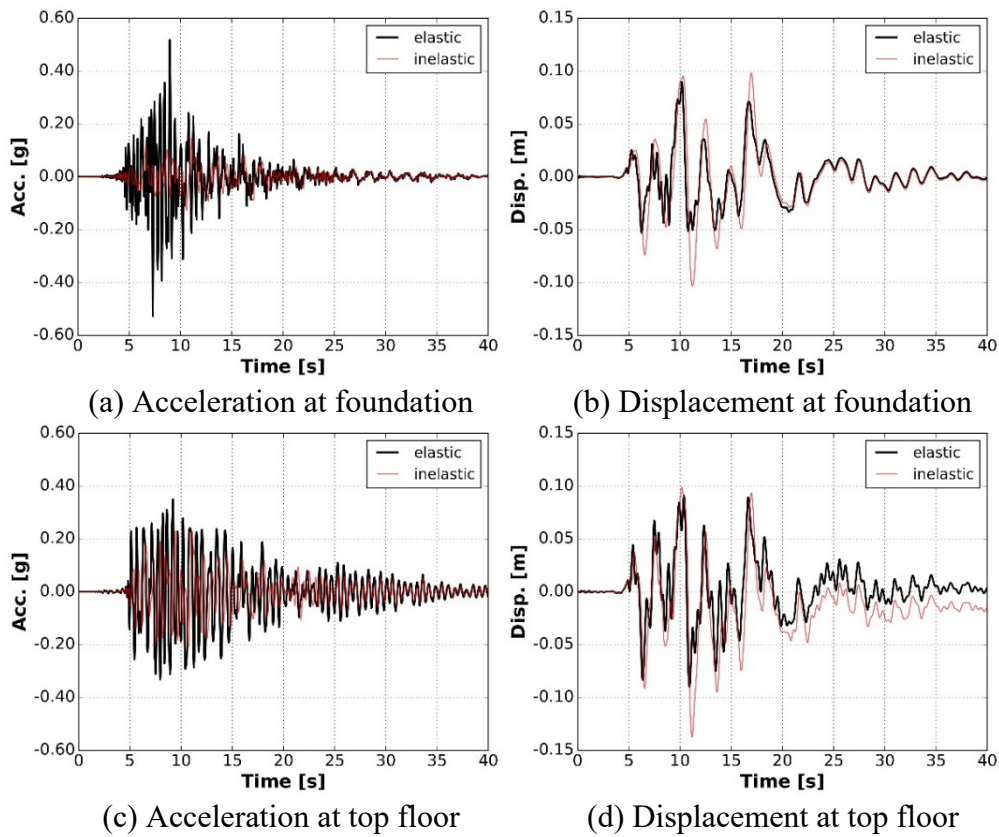


Figure 7: Dynamic responses of the steel building model.

4.3 Plastic Energy Dissipation

Figure 8 presents the distribution of plastic dissipation density in the SSI model. Note

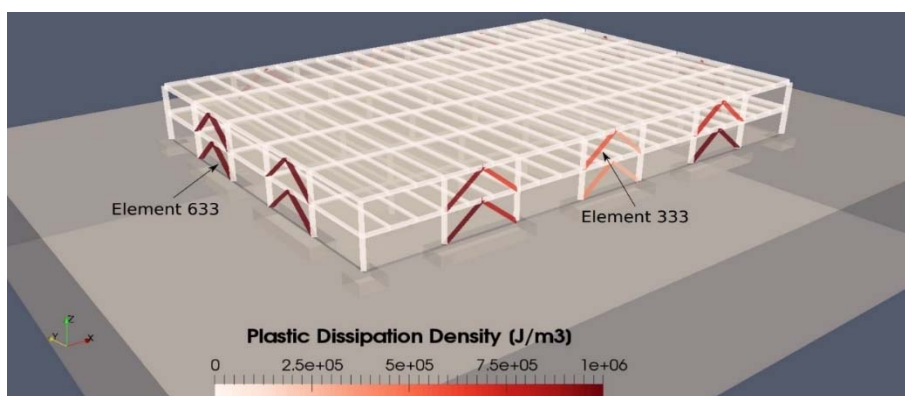


Figure 8: Distribution of plastic dissipation density in the SSI model.

that the plastic dissipation density in the BRB elements are significantly higher than that in the other components. This means that the majority of seismic energy is

dissipated in the BRBs, indicating that they are indeed effective in seismic protection of structures.

Another interesting observation is that the amount of plastic dissipation accumulated in each BRB is very different. For example, as highlighted in Figure 8, Element 633 dissipates much more seismic energy than Element 333. Figure 9 further illustrates this difference by directly comparing the evolution of plastic dissipation density in these two elements. It can be seen that Element 633 dissipates almost 10 times more seismic energy than Element 333.

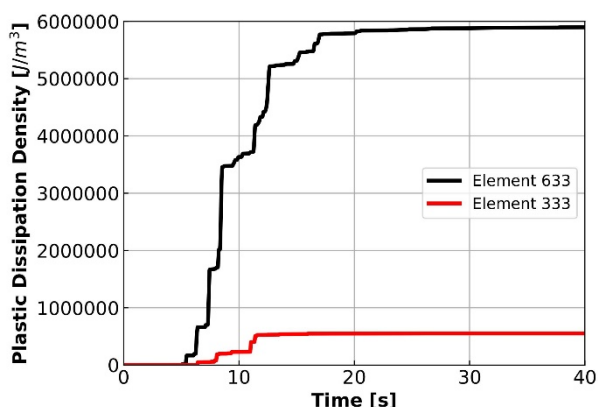


Figure 9: Evolution of plastic dissipation density for two BRB elements.

It should be mentioned that all BRBs in the SSI model are designed to be the same, per current engineering practice. However, the observation made in Figure 8 and 9 indicates that the seismic demand of a BRB differs depending on its location. According to Figure 8, the BRBs located along the short side of the structure tends to accumulate more plastic dissipation than those along the long side. This is not surprising since there are fewer BRBs along the short side thus each dissipates more energy. Another observation is that among the six BRBs along the long side, the middle ones show significantly less plastic dissipation. Further investigation is required to elucidate the correlation between the location and the seismic demand of BRBs in a structure.

4 Conclusions

This paper presents a numerical study on the seismic performance of a low-rise steel structure with BRBs. Focus is on the plastic dissipation accumulated in the BRBs during a seismic event. The energy computation approach developed in previous studies is summarized. The modelling procedure of the SSI system containing the two-story steel building is discussed with relevant details. Eigen analysis results, dynamic responses, and energy analysis results are presented and discussed.

Looking at the acceleration and displacement responses of the numerical model, it is not clear whether the BRBs installed in the structure are effective in terms of seismic protection. On the other hand, the energy analysis clearly shows significant seismic energy dissipation in the BRB elements, proving their effectiveness. This illustrates

the advantage of using energy-based concepts and parameters, particularly plastic dissipation, in seismic performance analysis.

Another interesting finding is that the BRBs dissipate different amounts of seismic energy when installed at different locations. It is suggested that a detailed nonlinear numerical analysis should be conducted to determine the location-dependent seismic demand of a structure. This could provide important information for the design and positioning of BRBs, improving the overall safety and economy of infrastructure objects.

References

- [1] C.J. Black, N. Makris, I.D. Aiken, “Component testing, seismic evaluation and characterization of buckling-restrained braces”, *Journal of Structural Engineering*, 130(6), 880-894, 2004. [https://doi.org/10.1061/\(ASCE\)0733-9445\(2004\)130:6\(880\)](https://doi.org/10.1061/(ASCE)0733-9445(2004)130:6(880)).
- [2] Y. Zhou, H. Shao, Y. Cao, E.M. Lui, “Application of buckling-restrained braces to earthquake-resistant design of buildings: A review”, *Engineering Structures*, 246, 112991, 2021. <https://doi.org/10.1016/j.engstruct.2021.112991>.
- [3] G. Papazafeiropoulos, V. Plevris, M. Papadrakakis, “A new energy-based structural design optimization concept under seismic actions”, *Frontiers in Built Environment*, 3, 44, 2017. <https://doi.org/10.3389/fbuil.2017.00044>.
- [4] H. Yang, H. Wang, B. Jeremić, “An energy-based analysis framework for soil structure interaction systems”, *Computers & Structures*, 265, 106758, 2022. <https://doi.org/10.1016/j.compstruc.2022.106758>.
- [5] H. Yang, H. Wang, Y. Feng, F. Wang, B. Jeremić, “Energy dissipation in solids due to material inelasticity, viscous coupling, and algorithmic damping”, *Journal of Engineering Mechanics*, 145(9), 04019060, 2019. [https://doi.org/10.1061/\(ASCE\)EM.1943-7889.0001617](https://doi.org/10.1061/(ASCE)EM.1943-7889.0001617).
- [6] J.F. Hall, “Problems encountered from the use (or misuse) of Rayleigh damping”, *Earthquake Engineering & Structural Dynamics*, 35(5), 525-545, 2006. <https://doi.org/10.1002/eqe.541>.
- [7] B. Jeremić, G. Jie, Z. Cheng, N. Tafazzoli, P. Tasiopoulou, F. Pisanò, J. Abell, K. Watanabe, Y. Feng, S.K. Sinha, F. Behbehani, H. Yang, H. Wang, “The RealESSI Simulator System”, University of California, Davis, USA, 1988-2023. <http://realessi.info/>.
- [8] H. Yang, S.K. Sinha, Y. Feng, D.B. McCallen, B. Jeremić, “Energy dissipation analysis of elastic-plastic materials”, *Computer Methods in Applied Mechanics and Engineering*, 331, 309-326, 2018. <https://doi.org/10.1016/j.cma.2017.11.009>.
- [9] H. Yang, H. Wang, Y. Feng, B. Jeremić, “Plastic Energy Dissipation in Pressure-Dependent Materials”, *Journal of Engineering Mechanics*, 146(3), 1-9, 2020. [https://doi.org/10.1061/\(ASCE\)EM.1943-7889.0001728](https://doi.org/10.1061/(ASCE)EM.1943-7889.0001728).
- [10] H. Yang, Y. Feng, H. Wang, B. Jeremić, “Energy dissipation analysis for inelastic reinforced concrete and steel beam-columns”, *Engineering Structures*, 197, 109431, 2019. <https://doi.org/10.1016/j.engstruct.2019.109431>.

- [11] M. Menegotto, P.E. Pinto, “Method of analysis for cyclically loaded reinforced concrete plane frames including changes in geometry and non-elastic behaviour of elements under combined normal force and bending”, in “IABSE Symposium on Resistance and Ultimate Deformability of Structures Acted on by Well Defined Repeated Loads”, Lisbon, Portugal, 15-22, 1973.
- [12] F.C. Filippou, V.V. Bertero, E.P. Popov, “Effects of bond deterioration on hysteretic behavior of reinforced concrete joints”, Earthquake Engineering Research Center, University of California, Berkeley, USA, 137-147, 1983.
- [13] J. Bielak, K. Loukakis, Y. Hisada, C. Yoshimura, “Domain reduction method for three-dimensional earthquake modeling in localized regions. part I: Theory”, Bulletin of the Seismological Society of America, 93(2), 817-24, 2003. <https://doi.org/10.1785/0120010251>.
- [14] H. Wang, H. Yang, Y. Feng, B. Jeremić, “Modeling and simulation of earthquake soil structure interaction excited by inclined seismic waves”, Soil Dynamics and Earthquake Engineering, 146, 106720, 2021. <https://doi.org/10.1016/j.soildyn.2021.106720>.